Unravelling the energy transfer of Er^{3+}-self-sensitized upconversion in Er^{3+}–Yb^{3+}–Er^{3+} clustered core@shell nanoparticles

Bolong Huang*[1], Mingzi Sun[1], Alan William Dougherty[2], Hao Dong[3], Yue-Jiao Xu[3], Ling-Dong Sun*[3], Chun-Hua Yan*[3]

1. *Department of Applied Biology and Chemical Technology, The Hong Kong Polytechnic University, Hong Hum, Kowloon, Hong Kong SAR, China.*
2. *Department of Computing, The Hong Kong Polytechnic University, Hong Hum, Kowloon, Hong Kong SAR, China.*
3. *Beijing National Laboratory for Molecular Sciences, State Key Laboratory of Rare Earth Materials Chemistry and Applications, PKU-HKU Joint Laboratory in Rare Earth Materials and Bioinorganic Chemistry, College of Chemistry and Molecular Engineering, Peking University, Beijing 100871, China.*

*Email: bhuang@polyu.edu.hk (BH); sun@pku.edu.cn (LDS); yan@pku.edu.cn (CHY)

Abstract

Unravelling upconversion (UC) energy transfer mechanism is significant for designing novel efficient anti-Stokes phosphors. We have studied correlation of different lanthanide dopants within the Er^{3+}-self-sensitized core@shell upconversion nanoparticles (UCNPs). Here in this work, our focus will be those high concentration dopants that are enough to produce the clustering effect, especially to the interplay between Er^{3+} and Yb^{3+}. We demonstrate that whatever is the amount of the self-sensitizer (e.g. Er^{3+}), the abnormal absorption enhancement will occur as long as the clustering Yb^{3+} is present. This effect originates from substantial energy transfer between Yb^{3+}-Yb^{3+} clusters despite the increased energy back transfer from Yb^{3+} to Er^{3+}. Therefore, the energy transfer efficiency is still constrained. However, we conversely used one of the aforementioned quench-paths of UC energy transfer, to easily transfer the energy from the in-shell shell layer to the in-core area with assistance of energy potential reservoir, which was given by the homogeneous core@shell band offset at the interface region. Indirectly, we actualize the Er^{3+} UC luminescence with self-sensitization through an extended energy transfer path. This work provides a solid support and analytic theory for unraveling the energy transfer mechanism form recent works on Er^{3+} self-sensitized UC luminescence.

Introduction

Since last decades, considerable efforts have been made on flexible modulations of the UC emissions, which have always been a big concern in either organic or inorganic rare-earth systems [1-6]. As summarized by literatures [2, 7-9], the manipulations of UC emissions mainly develop towards two trends: (a) to enhance the UC efficiency and (b) to regulate the output colors. The synthesis strategies have been implemented into the tunability on the lanthanides nanocrystals (NCs) or other forms of nanoparticles (NPs) through as thermal decomposition, hydro(solvo)thermal method etc [7, 8]. The synthesized alpha- (cubic) and beta- (hexagonal) phased alkali rare-earth (RE) fluoride NCs, such as $NaYF_4$ and $NaGdF_4$, are therefore of particular interest in fields of highly efficient UC luminescence [1] due to lower rate of photo-induced charge carrier recombination and higher efficiency for energy transfer.

Native energy transfers in Ln^{3+}-doped UCNPs dominate the UC efficiency and emission output [10]. The UC emission will significantly improve through an increased efficiency of energy transfer under external excitation. Since different energy transfer pathways via various mechanisms of electronic transitions might lead to tunable output color of UC emissions [12], development on high-throughput synthesis and screening for applicable candidate UCNPs still restricts in conventional experimental trial pattern without specific direction [11]. Therefore, it is necessary to investigate the theoretical energy transfer mechanism for guidance on manipulation of the UC.

Among of them, core-shell engineered Lanthanide(Ln) NPs are one of the best achievable approaches [13-15]. A perfect epitaxial shell layer plays a key role in blocking or suppressing the channels of energy transfer from UC activator to surface quenching sites (e.g. defects, impurities, solvent molecules, and capping ligands) on the core. Recent energy migration-mediated upconversion (EMU) experiments show the synthesized core-shell NPs have excellent efficiencies in tunable luminescence [13-15].

The development of novel controllable and energy efficient UC luminescence materials is highly desired in the field of luminescence science. Tailorable core-shell nanostructured Ln materials demonstrate tremendous potential in this regard due to their ~~novel~~ unique 4f-orbtial electronic structures. To improve the luminescence performance, extensive studies on UC energy transfer route-maps and mechanisms are required. Quenching effects between luminescence centers in bulk phase of Ln luminescent materials are usually the dominant reasons for low efficiency of the energy transfer for UC luminescence. These quenchers are assisted by the phonons or intrinsic defects in the bulk-sized Ln materials, which are thermodynamically stable with high concentrations. Conversely, the surface effects will become stronger and dominate for the Ln UC luminescence in nanoparticles (UCNPs) due to the more evident quenching effect caused by surface lattice relaxation and absorbing ligands [16]. Hence, it is worthy considering that, the overall downgrade of the luminescence intensity can be mainly attributed to the surface quenching effect. Such effect will affect both the energy transfer between luminescence centers in the near-surface region and the activation centers in NPs. Therefore, extensive studies to find out the quenching-prohibition and related mechanism is the key to increase the UC luminescence efficiency.

Based on our recent works [7, 10, 17, 18], two mechanisms are potentially influencing the enhancement of the efficiency for core-shell UCNPs: (1) the impact of the in-shell dopant

concentration effect, and (2) the correlations between local surface structures and corresponding intrinsic quenchers. For the mechanism-(1), the highly concentrated dopants within the shell layer can enhance the emission intensity with enlarged absorption cross-section. But it may also lower down the intensity by quenching the luminescence center *via* continuous non-radiative multiphoton cross-relaxation channels among sensitizers. Therefore, mechanism-(1) is a dilemma that restricts researchers with the selection on dopants [8, 18]. While for the mechanism-(2), the NP surface usually shows relatively low crystallization-degree with much the surface lattice defect and relaxation, which could assist the surface quenching effect of the luminescence centers. It has been indicated that the UC luminescence intensity can be enhanced by coating the non-doped shell layer because the distance between surface and luminescence center has increased [17, 19, 20] and meanwhile, the surface quenching is also suppressed. Regarding these two different mechanisms, we address another discussion point that whether the arisen surface quenching effect will be simultaneously annihilated with increased thickness of non-doped shell layer.

The core-shell nanostructure was originally imported for enhancing the UC efficiency with a higher quantum yield [21]. A uniformly epitaxial grown shell over the core can effectively block the energy transfer from activator (RE-dopant ion) sites in the core to surface defects, capping ligands, and solvent molecules [7, 22, 23]. With developed synthesis, the original role of shell is no longer to just be the passivation, and it can also accommodate the RE-ion doping and efficiently transfer the energy from the core to the shell to tune the color [3, 14, 24] or intensity of output UC luminescence [13, 25]. Accordingly, core-shell nanostructural engineering introduces a new variable (core-shell recombination) into UC materials design. A recent quantum yield of core-shell $LiLnF_4$ remarkably approaches to ~7% [26] with new route and strategy of alkali elements choices.

In general, a designated synthesis with selective chemical doping is an effective strategy to modify the electronic structure and surface property of UCNPs such that their performance can be significantly improved [6, 22, 27-29]. In detail combining with specific conditions of synthesis, the appropriate tuned dopant/trap levels within single- or multi-shell [3, 13, 14] by layer-by-layer epitaxial growth, precisely control of shell thickness or surface coating in the core-shell nanostructure [15, 17, 19, 30, 31] have been attempted out for controlling the required output UC luminescent properties. For the shell thickness impact [17, 19, 20], both homogenous and heterogeneous shell can passivate the surface quenching state on the core effectively [7]. The perfect epitaxial growth of layer-by-layer multi-shell [31] can be distinguished from the core via various matured experimental techniques [19, 32-34].

Nevertheless, with recent gradually concentrated on the interface [35-38], exact theoretical guiding mechanism of energy transfer at the interface for UC luminescence in core-shell structure is still not perfectly clarified and established. Guided by our recently developed density functional theory (DFT) calculation method [39-41], we have carried out a preliminary exploration on the decaying process, quenching mechanism and energy transfer dynamics via experimental characterizations. As previous work showed, the heterogeneous core@shell system has an intrinsic obstacle for fully efficiently transferring the energy between the core and shell parts. This barrier is found as the interface bonding induced gap states (IBIGS) reported previously[42]. Either the real entities transport (electrons and holes) or the non-real entities (radiative or non-radiative resonant energy transfer, i.e. LRET or FRET) could be hindered by the interface wrong bonds. However, for the homogeneous core@shell system, there would be no wrong bonds or less IBIGS effects as found in heterogeneous system. It is necessary to investigate the inter-layer regional band offset for charge transfer and doping

concentration effect induced both enhancement and quenching effects. To dates, terminating the quenching sites is still the significant manner to improve the UC energy transfer efficiency. Here, we illustrate one of the possible quenching effects induced by increased doping concentration of lanthanide ions in the shell layer from core@shell system.

Conventionally, majority of previous works has been reached a consensus that the Yb^{3+} acts as sensitizer (S) while the activator (A) is for Er^{3+} (and Tm^{3+}/Ho^{3+}, *etc*.). The resonant upconverted energy is non-radiatively donated from Yb^{3+} onto the Er^{3+} site. Such energy transfer between S-A pair is traceable by amount of works according to our review [7]. Due to the energy level-matching between the transition of $^2F_{7/2}\rightarrow{}^2F_{5/2}$ (Yb^{3+}) and $^4I_{15/2}\rightarrow{}^4I_{11/2}$ (Er^{3+}), the resonant energy transfer efficiently occurs from Yb^{3+} to the Er^{3+}. The upward energy excitations are ongoing to $^4I_{11/2}\rightarrow{}^2F_{7/2}$ or $^4I_{13/2}\rightarrow{}^4F^{9/2}$ of Er^{3+}. With non-radiative relaxation, the subsequent green emissions are from $^2H_{11/2}$ and $^4S_{3/2}$ back to ground state of Er^{3+} ($^4I_{15/2}$), and the red emission of Er^{3+} is also achieved by de-excitation from $^4F_{9/2}\rightarrow{}^4I_{15/2}$. Such two-photon UC process induced green and red emissions can be obtained simultaneously.

Recently, high concentration doped Er^{3+} UC core@shell system has remarkably shown a role of sensitizer and achieve the UC red emission by self-sensitization[43], through an alleviation of concentration quenching. Moreover, Liu et al further show the sensitization of Er^{3+} can be achieved by an energy transfer between Er^{3+}-Er^{3+} pair via host intrinsic defect or impurity, especially to the Tm^{3+} dopant, which acts an energy confining effect to enhance such self-sensitization[44]. Therefore, the in-core UC energy transfer efficiency can reach higher by relative lower power density of excitation based on current crafted UC core@shell systems. With inspired by the work of Liu et al [45], high concentration Ln^{3+} can be realized by substituting the sub-lattice and gives a clustering effect [45]. This clustering effect is physically reasonable. Under equilibrium stage of synthesis, rich chemical potential may drive the dopant to be clustering within the host (e.g. β-$NaLnF_4$). Those Ln^{3+} dopant clusters will exhibit different absorption behaviors at the excited states. The consequent energy transfer for UC luminescence may be influenced and differed from the original path given by low-concentrated Ln^{3+} doping [4, 9, 46, 47]. We accordingly propose a new energy transfer map as illustrated in Figure 1 (a) with following routes:

Route-1: The highly doped Er_Y^{3+} clusters (i.e. Er substitutes Y-site) stabilize within the core host matrix, and gain external NIR-laser excitations.
Route-2: The excited energies will further be transferred onto the highly concentrated (Yb_Y^{3+}, Er_Y^{3+}) co-doped clusters within the shell region.
Route-3: Due to the abnormal absorption enhancement of Yb_Y^{3+} clusters, the energy UC will be continued from (Yb_Y^{3+}, Er_Y^{3+}) to Yb_Y^{3+} clusters in the shell layer.
Route-4: The upconverted energy at the Yb_Y^{3+} in the shell will be migrated backward to the ones within interface region, which is assisted by the the band-offset effect induced potential contrast between inter-layers.
Route-5: The excited electrons at higher levels of Yb_Y^{3+} clusters will be de-excited back to the lower levels of Er_Y^{3+} clusters, following with a secondary de-excitation from $^4F_{9/2}$ to $^4I_{15/2}$.

Finally, the self-sensitized red-emission is achieved via $Er^{3+}\rightarrow Yb^{3+}\rightarrow Er^{3+}$ along the above paths with assistance of interfacial band offset and abnormal enhanced absorption.

Figure 1 (b) schematically demonstrates the dilemma of highly doped sensitizer in the shell. This dilemma means that it cannot only enhance the UC efficiency by larger absorption cross-section, but also suppress the energy transfer from sensitizer to activator (i.e. S-to-S

instead of S-to-A). In addition, over-suppression is ongoing to transfer the UC energy towards the surface quencher via the energy depletion channels. Figure 1 (c) illustrates the energy transfer between Yb^{3+} clusters are energetically favorable while there the energy barrier is facing at the path from Er^{3+} to Yb^{3+} clusters. This arises because the Yb^{3+} usually has larger absorption cross-section than the one in Er^{3+}. The process occurred via routes (2, 3, 4, and 5), especially to the route 4 and 5, can suppress the energy transfer from Yb_Y^{3+} cluster in the shell to the surface quenching centers as schematically elucidated in Figure 1 (d). This will rely on our designed energy transfer paths achieved by controlled doping within selected area at specific concentrations. The morphology is also a key to modulate the interfacial band offsets, in order to yield a contrast in chemical potentials between shell and core regions. With this design, the energy depletion channel from in-shell Yb_Y^{3+} cluster to surface quenchers is accordingly suppressed, and the UC luminescence efficiency is subsequently improved to a higher extent.

Herein we argued two key points: (1) whatever the amount of the sensitizer dopant increased (e.g. Er_Y^{3+}), as long as the Yb_Y^{3+} doped, the abnormal absorption enhancement will always occur and the substantial (evident) energy transfer from Yb_Y^{3+} to Yb_Y^{3+} remained unchanged rather than the backward transfer from Yb_Y^{3+} to Er_Y^{3+}. Therefore, the energy transfer efficiency is still constrained. (2) However, as illustrated in Figure 1, if we used the routes (1-to-5) of UC energy transfer, the excited energy will be easily transferred from the shell to core region by the homogeneous core@shell band offset at the interface region. This arises because the interfacial non-crystalization within that system will form a constant potential contrast. Indirectly, we actualize the newer $Er^{3+} \rightarrow Yb^{3+} \rightarrow Er^{3+}$ transfer through an extended energy transfer path. This work provides a solid support and analytic theory for unraveling the energy transfer mechanism form our recent work on Er^{3+} self-sensitized UC luminescence.

Calculation setup

For calculation of electronic properties at the ground states, the density functional theory (DFT) calculation has been carried out. We used the CASTEP source code to perform calculations with DFT+U method [48]. The hexagonal lattice with the $P\bar{6}$ space group is modeled for β-phase $NaLnF_4$ (Ln=Y, Er, and Tm). The Na, Y, Er, Tm and F norm-conserving pseudopotentials are generated using the OPIUM code in the Kleinman-Bylander projector form [49], and the non-linear partial core correction[50] and a scalar relativistic averaging scheme [51] are used to treat the spin-orbital coupling effect. In particular, we treated the (4*f,* 5*s*, 5*p*, 5*d*, 6*s*) states as the valence states of the Er and Tm atoms. The RRKJ method is chosen for the optimization of the pseudopotentials [52].

For the all of the electronic states calculations in β-$NaLnF_4$ (Ln=Y, Er, and Tm), we use the self-consistent determination for the U correction on the localized 4f orbitals to correct the on-site Coulomb energy of the electron spurious self-energy. In previous work, we have estalished a manner to determine the on-site electronic self-energy and related wavefunction relaxation in the semicore d or f orbitals in heavy elements with mixed valence, so as to obtained an accurate orbital eivenvalues for electronic structures and transition levels [39-41, 53-59]. It is ab-initio two-way crossover searching calculations by two different functionally compiled CASTEP-17 developing source codes[40, 44, 60]. The detail process was referred to the previous work, and the schematic theoretical determination process is demonstrated in Figure 2. With our self-consistently determination process, the on-site Hubbard U parameters for 4f of Er and Tm and different 2p of F-sites are obtained respectively. Time-dependent DFT calculation has been further performed with two-electron based Tamm-Dancoff

approximation [61] imported from our self-consistently corrected ground state wavefunctions, which is significant for two-photon absorption (TPA) calculations.

Further on the excited states, the related calculations for β-$NaLnF_4$ doped with different trivalent lanthanide ions (Ln^{3+}, from La to Lu) were examined by a series of TD-DFT calculations. These excitation energies correspond to the locations of the absorption peaks in the optical spectrum of a material and are more accurate than Kohn-Sham excitation energies. Some of the de-excitation paths between different energy levels correspond to the emission peaks from the output luminescence spectrum. The calculations were performed using the Tamm-Dankoff approximation [61]. This method allows us to calculate the full set of optical properties with support of the excitation energies and corresponding transition probabilities. This study is also applicable to low-dimensional $NaLnF_4$ systems, as extra effects such as boundary effects, quantum-confinement effects, and different coordination-induced mixed-valence effects are necessarily taken into account.

Results and discussion

Here we start to discuss different UC properties induced by the clustering effect regarding the Er_Y^{3+} single-dopant and (Er_Y^{3+}, Tm_Y^{3+}) co-dopants. With developed TD-DFT code imbedded by the self-consistent orbital correction, the fine levels of excited states for β-$NaYF_4$ with Ln^{3+} doped systems (Ln= Gd, Tb, Dy, Ho, Er, Tm, and Yb) have been extensively calculated (Figure 3). (Note, the relative error has been reduced into the magnitude of ~0.2 eV). At thermodynamic equilibrium stage, these high concentration dopants will form themselves into a cluster and locally aggregate within the Y sub-lattice. We name them as single-dopant-cluster (SDC) and co-dopant-cluster (CDC) by the type of doping, respectively.

Without Tm_Y^{3+} co-doping, we see the β-$NaYF_4$:Er_Y^{3+} (SDC) system can accommodate a two-photon-absorption (TPA) scheme for exciting the electrons from the Er_Y^{3+} center to a higher excited state. Actually, there has been reported that the Er^{3+} itself can achieve UC luminescence *via* multi-photon absorption (MPA) of 1490 nm pump photons [62]. From the excited energy levels, the energetic interval of such TPA process is quite un-evenly distributed. This induces the TPA process for the first step excitation requires an over too large energy gap to pump-up the excited electrons to the higher states.

In the case of (Er_Y^{3+}, Tm_Y^{3+}) CDC within β-$NaYF_4$, the energy intervals of TPA process is relatively reduced and the medium-energy-range (MER, 1~2.5 eV) excitation levels can be seen to be more evenly distributed than the system without Tm-doping. We confirm that, the (Er_Y^{3+}, Tm_Y^{3+}) CDC system induces rather low excitation energy and with even higher probability for accommodating the excited electrons, where are shown in the energy of 0.5~1.0 eV from Figure 3 (a). Moreover, the original excitation energy gap within the MER scale is filled with more excitation energy levels with substantially high-participated Tm_Y^{3+} ions within the (Er_Y^{3+}, Tm_Y^{3+}) CDC system. Recent experiment shows that Tm_{Ln}^{3+} doped $NaLnF_4$:Er^{3+} enhanced the Er^{3+}-self-sensitization for the experimentally observed ~650 nm luminescence within near infra-red (NIR) range [43, 44]. This can be explained by our work that, with same TPA process, the Tm^{3+}-doped system reaches to an even higher energy state near the 2 eV. This process spontaneously results in an energy relaxation from higher to lower energy levels of Er_Y^{3+} center. Thus, more excited electrons are accumulated to the Er_Y^{3+}-activator-sites and an enhanced probability with less energy barrier of TPA is achieved.

The calculated relative oscillator strengths are compared between two systems (Figure 3 (b)), and find the Tm_Y^{3+} system re-aligns the absorptions for the UC. The excited electrons on these states are more evenly resonating and the absorption intensity turns to be overall higher than the system without Tm doping. This comparison further implies that, the Tm-doping reduces the energy barrier and merges more energy sourced from the host lattice. This will support the pumping-up the electrons to a higher state with a higher efficiency reached.

We move on to other lanthanide dopants within the core@shell system. The Figure 3 (a) shows the excited energy of the interfering effects on the excited energy levels by these clustered co-dopants in the homogeneous core@shell system. In the single-dopant cases, Yb_Y^{3+} SDC has the relatively lower absorption energy level (first excited energy level) than the one found in Er_Y^{3+} SDC. The (Er_Y^{3+}, Tm_Y^{3+}) CDC also has the lower absorption energy than the Er_Y^{3+} SDC, and close to the level of Yb_Y^{3+} SDC. Considering the (Er^{3+}, Yb^{3+}) CDC, this case presents similar absorption level to the Yb_Y^{3+} SDC only with about 0.2 eV higher.

Figure 3 (b) shows that, the (Er^{3+}, Yb^{3+}) CDC in the core@shell system exists excitated energy absorption abnormality, showing a stronger oscillator strength at the energy level lower than the those of Er^{3+} dopant levels. The higher excited energy levels of Yb_Y^{3+} SDC shows the resonating virtual energy level high lying near 3.0 eV, in a good agreement with previous reported by Liu et al [45]. In that system, violet UC emission is obtained by high concentration of doping by (Yb^{3+}, Er^{3+}) which has subsequently clustered within the host matrix (KYb_2F_7) [45]. The high absorbed excited energy level is lined with a virtual levels forming-up by Yb_Y^{3+} SDC proposed in our work, similar to the ones in cooperative energy transfer (CET) summarized previously[7].

As we know, the probability of energy absorption and upconversion transfer is monotonically increased with the strength of the oscillator strengths. The contrast in the oscillator strengths points out the most probable trend of energy transfer between SDSs or CDCs. If the Er_Y^{3+} SDC is firstly excited by the external NIR laser source, the energy absorption can be achieved by the TPA process. The Er_Y^{3+} SDC will further transfer the excited energy from higher to lower energy levels but with weaker to stronger oscillator strengths. Such trend of energy transfer can be reflected from Er_Y^{3+} SDC to (Er^{3+}, Yb^{3+}) CDC (i.e. route-2 from Figure 1 (a)).

This process arises because the pure Er_Y^{3+} SDC energy transfer induced self-sensitization for UC luminescence has relative low efficiency than the assistance of other RE^{3+}. As previous collaborative work shows this energy transfer must be assisted by an energy agglomeration center such as Tm^{3+} [44]. Accordingly, the Er_Y^{3+} SDC will firstly transfer the energy absorbed from the external excitation to the (Er^{3+}, Yb^{3+}) CDC center for further upconverted energy transfer to higher levels under multi-photon absorption process (MPA) given by continuous NIR laser pumping source. Further shown in Figure 3 (c) that, the Yb_Y^{3+} SDC has rather strong oscillator strength which means the probability of energy absorption of external excitation is nearly four times higher than the (Er^{3+}, Yb^{3+}) CDC absorption. This abnormality in contrast leads to a continuous process that, the energy transfer is further ongoing to be upconverted to a higher energy level that Yb_Y^{3+} SDC occupied.

With increased doping concentration of Yb^{3+} within the shell layer, the Yb^{3+} tends to aggregate nearby each other and form the SDC. The Yb_Y^{3+} SDC will quench the energy transfer among the medium energy range (MER) of UC luminescence. There will be also a trend to upconvert the absorbed energy towards rather high energy levels (above 2.5 eV), under the MPA laser stimulation. The lifetime of the UC luminescence at the MER will be

consequently shortened and the quantum yield will also be lowered. According to our analysis above, this negative effect has evidently been far beyond the positive contribution of Yb^{3+} concentration dependent energy absorption, resulting in a decreased intensity of UC luminescence.

However, the quenching effect discussed above can be conversely utilized as another positive effect for enhancing the energy transfer along a different path, as proposed in Figure 1. If Yb_Y^{3+} SDC locates within the interface region, local non-crystallizations loose the parity-forbidden 4f-4f transition. Meanwhile, the interface region with certain non-crystallizations can be also found in homogeneous core@shell system (Figure 4 (a) and (b)), since the local symmetry is different between core and shell layers. We find the system with such region possesses an evident and nearly constant valence and conduction band offsets, shown as VBO and CBO in Figure 4 (c) and (d). Recall the works reported by Dorenbos et al [63-65], among over 10000 host materials, inter-energetic distance between the lanthanide ions 4f levels and valence band maximum (VBM) is almost fixed. The only difference can be reflected by the energetic intervals between the 4f state and conduction band minimum (CBM), as well as the vacuum level of 4f state given by the Ln^{3+} dopants. Considering the existence of constant VBO and CBO, the Ln^{3+} ion levels is accordingly shifted, in which the lower symmetry can undertake the energy transfer from other layer [39]. Then the energy from the shell to core region between inter Yb_Y^{3+} SDC is transferable with the interface band offset.

On the other hand, the 4f state charge transfer can be also considered as a support for the UC luminescence energy transfer from the (Host:RE_1^{3+}) to (Host:RE_2^{3+}). Although the screening constant is large for lanthanide ions (Ln^{3+}, Ln=La…Lu) but still less than one where the "lanthanide-contraction" found [66]. Previous work demonstrated such physicochemical trend [41]. Following on the electron transfer, some inter-ionic unknown redox process can be interpreted as local charge transfer between RE^{3+} and host [67]. Therefore, the 4f level in the band gap is significant that overlaps with the host defects states. Further from previous report [42], the IBIGS influences the ETU [4, 46] efficiency for UC luminescence. We have preliminarily discussed a "structural selection rule" assisted by the occurrence of the interface from the core@shell system [39]. The different local symmetry of the *P-6* symmetry lattice arises because of the different local coordination of the fluoride (F) site in β-$NaLnF_4$ (Ln=Y, La…Lu). The energy transfers along the path from low to high symmetrical host lattice matrix [39]. The broken symmetry at the interface of homogeneous β-$NaYF_4$ allows transitions near the CB via the 5d→5d and 4f→4f simultaneously. Thus, the electronic relaxations for both dopant and host have been discussed.

With further cross-section relaxation along the same 4f excited energy level but under the different vacuum level of two Yb_Y^{3+} SDCs staying within two different regions, i.e. shell-layer and interface region, respectively. The difference in vacuum level that is produced by the band offsets is a perfect chemical potential contrast for 4f electrons of these two Yb_Y^{3+} SDCs at these two areas. The subsequent energy transfer actualized simply follows the trend from high chemical potential to lower levels. Therefore, a directed propagation of energy transfer via a contrast of chemical potential for those 4f-electrons staying at the same excited state energy levels belonging two different Yb_Y^{3+} SDCs (at shell and interface, respectively). The energy can be thus transferred from the shell into the core through the interface region.

Conclusion

In summary, we have analyzed the aforementioned quench-path of UC luminescence and reflect one important phenonmenon that Yb^{3+} dopant is the dominated reason of determining the abnormal absorption enhancement rather than the concentration of the sensitizer dopant (e.g. Er^{3+}). Instead of transferring energy back from Yb^{3+} to Er^{3+}, the substantial energy transfer from Yb^{3+} to Yb^{3+} will sustain. Therefore,within a core@shell system, high concentrated Er^{3+} and Yb^{3+} co-dopant clusters constraint the efficiency for energy transfer upconversion (ETU).

To highlight in this work, we utilize one quench-path of UC energy transfer to successfully design a new converse energy transfer pathway from the in-shell layer to the in-core area with assistance of energy potential reservoir given by the homogeneous core@shell band offset at the interface region. As a result, the Er^{3+} UC luminescence with self-sensitization has been realized indirectly through an extended energy transfer path, which afford a solid support by analytic theory on our recent work on Er^{3+} self-sensitized UC luminescence that illustrate the energy transfer mechanism.

Acknowledgement

This work was supported by NSFC (Nos. 21425101, 21590791, 21371011, 21331001) and MOST of China (2014CB643800). The author BH gratefully acknowledges the support of the Natural Science Foundation of China (NSFC) for the Youth Scientist grant (Grant No. NSFC 11504309, 21771156), the initial start-up grant support from the Department General Research Fund (Dept. GRF) from ABCT in the Hong Kong Polytechnic University, and the Early Career Scheme (ECS) Fund (Grant No. PolyU 253026/16P) from the Research Grant Council (RGC) in Hong Kong.

Figure 1

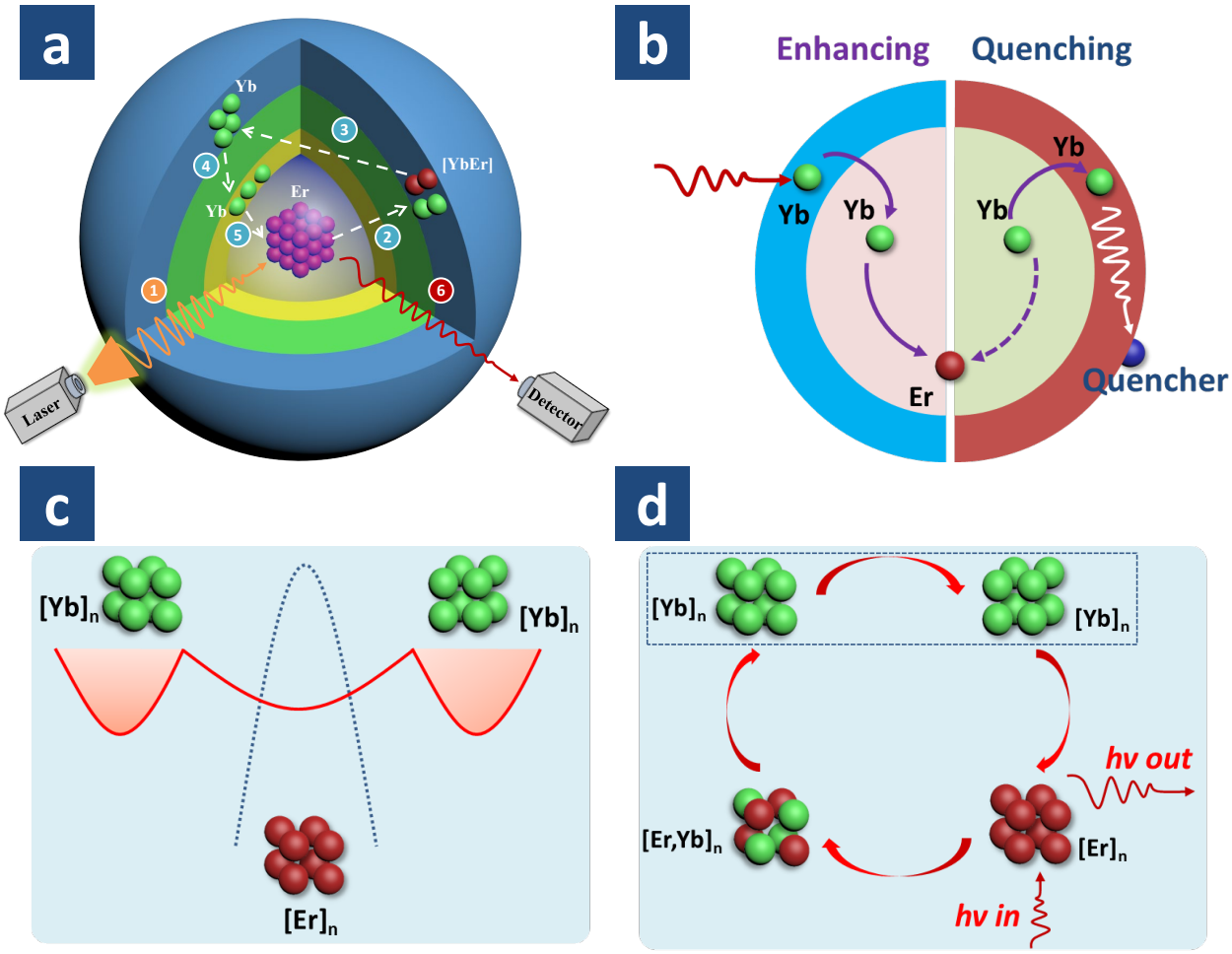

Figure 1. Schematic principle is shown for demonstrating the self-sensitized energy transfer route for subtle interplay on enhancing and quenching effects between Er^{3+} and Yb^{3+} dopant clusters. (a) The proposed new energy transfer map routes (1-to-5), and the self-sensitized red-emission is achieved via $Er^{3+}\rightarrow Yb^{3+}\rightarrow Er^{3+}$ along the above paths with assistance of interfacial band offset and abnormal enhanced absorption. (b) Schematic demonstration about the dilemma of highly doped sensitizer in the shell. This dilemma means that it cannot only enhance the UC efficiency by larger absorption cross-section, but also suppress the energy transfer from sensitizer to activator (i.e. S-to-S instead of S-to-A). (c) Illustration on the energy transfer between Yb^{3+} clusters are energetically favorable while there the energy barrier is facing at the path from Er^{3+} to Yb^{3+} clusters. (d) The process occurred via routes (2, 3, 4, and 5), especially to the route 4 and 5, can suppress the energy transfer from Yb_Y^{3+} cluster in the shell to the surface quenching centers The red-filled arrow represents the non-radiative resonant energy transfer (FRET) for output emission.

Figure 2

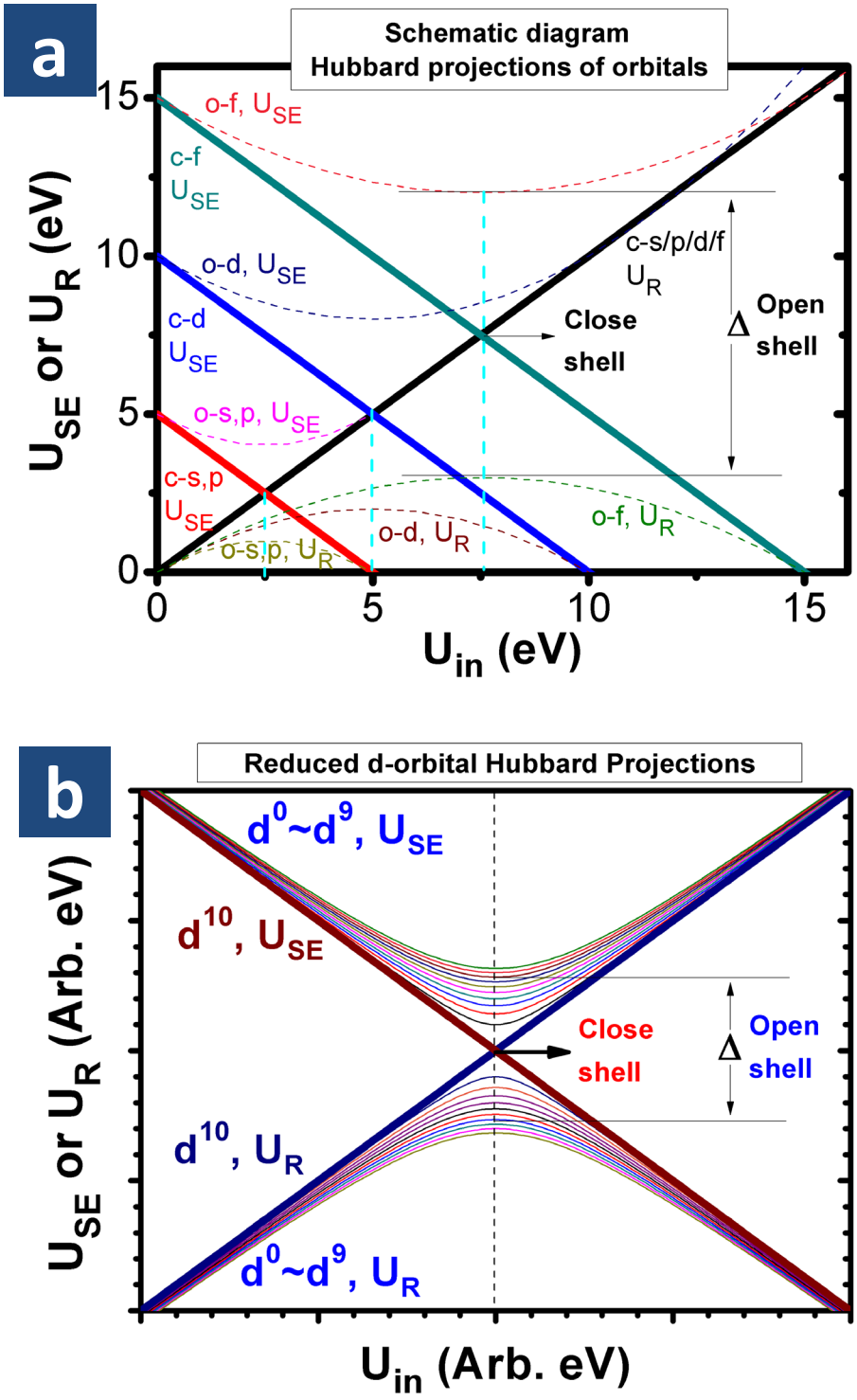

Figure 2. (a) Schematic diagram for the Hubbard projections of the self-energy and wavefunction relaxation of orbitals with different angular momentum (Lmax=0, 1, 2, 3). The crossover of self-energy and wavefunction relaxation are counteracted at the close-shell while with rigid non-zero shift Δ for open-shell situations. (b) Simplification of the schematic diagram for Hubbard potential projections of reduced d-orbitals. (U_{SE}= self-energy Hubbard

projection; U_R= wavefunction relaxation Hubbard projection; c= Close-shell; o= Open-shell; corrected U_{in}=horizontal axis of cyan line.).

Figure 3

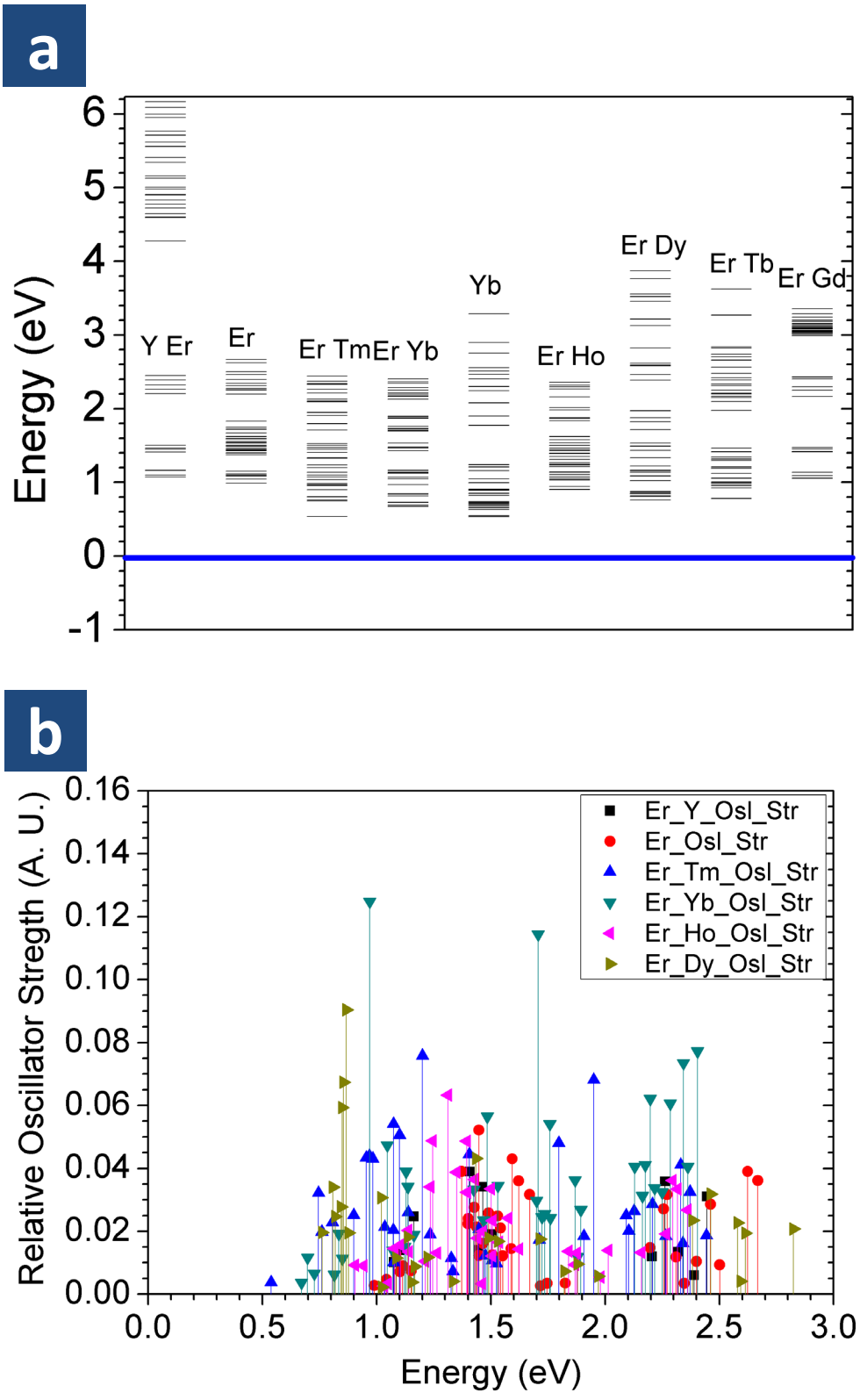

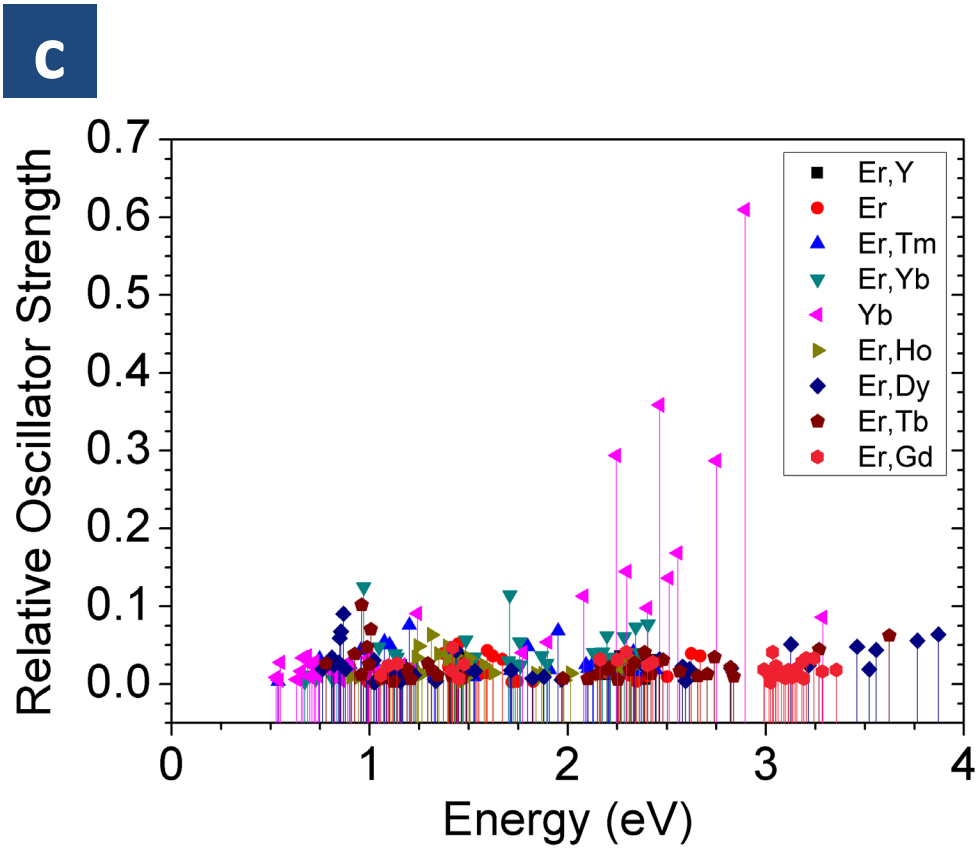

Figure 3. (a) Exited state energy levels of Ln^{3+} dopant clusters. (b) The relative oscillator strengths of dopant clusters. (c) Energy absorption abnormality induced by Yb^{3+} dopant clusters.

Figure 4

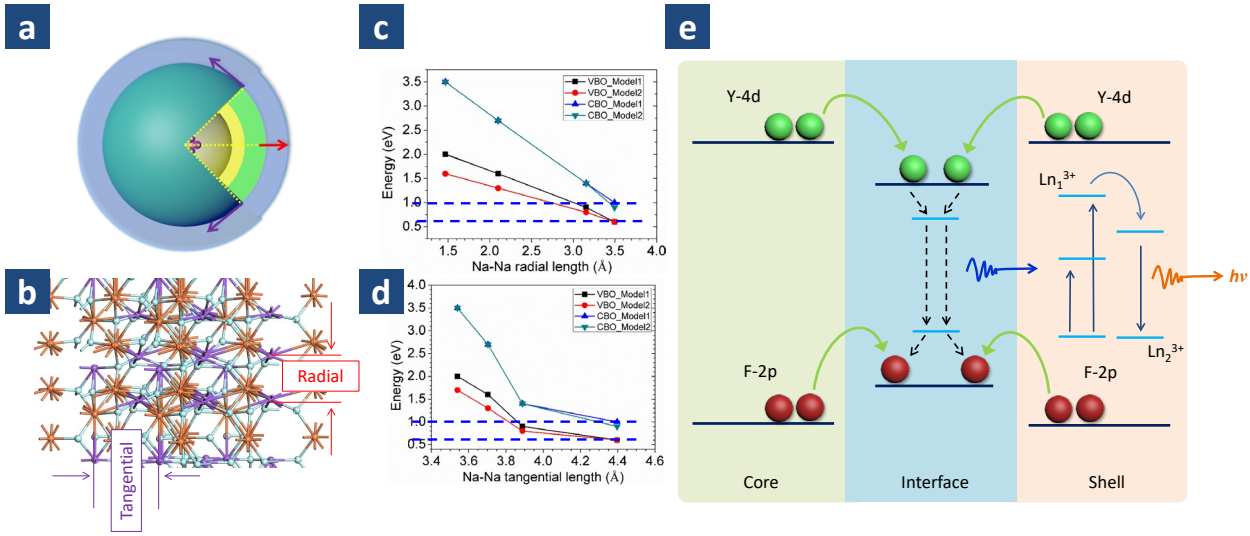

Figure 4. (a) Two principle directions for growth dynamics of core@shell UCNPs. (b) Local view on the host lattice of interface region from a core@shell system (β-$NaYF_4$). (c) Dependent behavior and convergence of band offsets with related to the radial length relaxation. (d) Dependent behavior and convergence of band offsets with related to the tangential length relaxation. (e) New type of band offsets mechanism existing within interface region induced by the radial and tangential lattice relaxations in homogenous core@shell system (β-$NaYF_4$).

References

1 X. Liu, C.-H. Yan, and J. A. Capobianco, *Chem. Soc. Rev.*, 2015, **44**, 1299.
2 F. Wang and X. Liu, *Chem. Soc. Rev.*, 2009, **38**, 976.
3 F. Wang and X. Liu, *Acc. Chem. Res.*, 2014, **47**, 1378.
4 F. Auzel, *Chem. Rev.*, 2004, **104**, 139.
5 J. Zhou, Q. Liu, W. Feng, Y. Sun, and F. Li, *Chem. Rev.*, 2015, **115**, 395.
6 G. Chen, H. Qiu, P. N. Prasad, and X. Chen, *Chem. Rev.*, 2014, **114**, 5161.
7 H. Dong, L.-D. Sun, and C.-H. Yan, *Chem. Soc. Rev.*, 2015, **44**, 1608.
8 L.-D. Sun, H. Dong, P.-Z. Zhang, and C.-H. Yan, *Annu. Rev. Phys. Chem.*, 2015, **66**, 619.
9 S. Gai, C. Li, P. Yang, and J. Lin, *Chem. Rev.*, 2014, **114**, 2343.
10 H. Dong, L.-D. Sun, and C.-H. Yan, *Nanoscale*, 2013, **5**, 5703.
11 E. M. Chan, G. Han, J. D. Goldberg, D. J. Gargas, A. D. Ostrowski, P. J. Schuck, B. E. Cohen, and D. J. Milliron, *Nano Lett.*, 2012, **12**, 3839.
12 L. Tu, X. Liu, F. Wu, and H. Zhang, *Chem. Soc. Rev.*, 2015, **44**, 1331.
13 F. Wang, R. Deng, J. Wang, Q. Wang, Y. Han, H. Zhu, X. Chen, and X. Liu, *Nat. Mater.*, 2011, **10**, 968.
14 R. Deng, F. Qin, R. Chen, W. Huang, M. Hong, and X. Liu, *Nat. Nanotechnol.*, 2015, **10**, 237.
15 Q. Su, et al., *J. Am. Chem. Soc.*, 2012, **134**, 20849.
16 N. Bogdan, F. Vetrone, G. A. Ozin, and J. A. Capobianco, *Nano Lett.*, 2011, **11**, 835.
17 Y.-F. Wang, L.-D. Sun, J.-W. Xiao, W. Feng, J.-C. Zhou, J. Shen, and C.-H. Yan, *Chem. –Eur. J.*, 2012, **18**, 5558.
18 L.-D. Sun, Y.-F. Wang, and C.-H. Yan, *Acc. Chem. Res.*, 2014, **47**, 1001.
19 F. Zhang, R. Che, X. Li, C. Yao, J. Yang, D. Shen, P. Hu, W. Li, and D. Zhao, *Nano Lett.*, 2012, **12**, 2852.
20 K. Prorok, A. Bednarkiewicz, B. Cichy, A. Gnach, M. Misiak, M. Sobczyk, and W. Strek, *Nanoscale*, 2014, **6**, 1855.
21 H.-X. Mai, Y.-W. Zhang, L.-D. Sun, and C.-H. Yan, *J. Phys. Chem. C*, 2007, **111**, 13721.
22 X. Chen, D. Peng, Q. Ju, and F. Wang, *Chem. Soc. Rev.*, 2015, **44**, 1318.
23 F. Wang, J. Wang, and X. Liu, *Angew. Chem. Int. Ed.*, 2010, **49**, 7456.
24 H. Dong, L.-D. Sun, W. Feng, Y. Gu, F. Li, and C.-H. Yan, *ACS Nano*, 2017, **11**, 3289.
25 B. Zhou, B. Shi, D. Jin, and X. Liu, *Nat. Nanotechnol.*, 2015, **10**, 924.
26 P. Huang, et al., *Angew. Chem. Int. Ed.*, 2014, **53**, 1252.
27 X. Li, F. Zhang, and D. Zhao, *Chem. Soc. Rev.*, 2015, **44**, 1346.
28 G. Chen, H. Agren, T. Y. Ohulchanskyy, and P. N. Prasad, *Chem. Soc. Rev.*, 2015, **44**, 1680.
29 A. Sedlmeier and H. H. Gorris, *Chem. Soc. Rev.*, 2015, **44**, 1526.
30 X. Li, D. Shen, J. Yang, C. Yao, R. Che, F. Zhang, and D. Zhao, *Chem. Mater.*, 2013, **25**, 106.
31 N. J. J. Johnson, A. Korinek, C. Dong, and F. C. J. M. van Veggel, *J. Am. Chem. Soc.*, 2012, **134**, 11068.
32 K. A. Abel, J.-C. Boyer, and F. C. J. M. v. Veggel, *J. Am. Chem. Soc.*, 2009, **131**, 14644.

33 K. A. Abel, J.-C. Boyer, C. M. Andrei, and F. C. J. M. van Veggel, *J. Phys. Chem. Lett.*, 2011, **2**, 185.
34 X. Liu, R. Deng, Y. Zhang, Y. Wang, H. Chang, L. Huang, and X. Liu, *Chem. Soc. Rev.*, 2015, **44**, 1479.
35 S. Han, X. Qin, Z. An, Y. Zhu, L. Liang, Y. Han, W. Huang, and X. Liu, *Nat. Commun.*, 2016, **7**, 13059.
36 X. Chen, L. Jin, W. Kong, T. Sun, W. Zhang, X. Liu, J. Fan, S. F. Yu, and F. Wang, *Nat. Commun.*, 2016, **7**, 10304.
37 B. Chen, D. Peng, X. Chen, X. Qiao, X. Fan, and F. Wang, *Angew. Chem. Int. Ed.*, 2015, **54**, 12788.
38 B. Zhou, L. Tao, Y. Chai, S. P. Lau, Q. Zhang, and Y. H. Tsang, *Angew. Chem. Int. Ed.*, 2016, **55**, 12356.
39 B. Huang, H. Dong, K.-L. Wong, L.-D. Sun, and C.-H. Yan, *J. Phys. Chem. C*, 2016, **120**, 18858.
40 B. Huang, *Phys. Chem. Chem. Phys.*, 2017, **19**, 8008.
41 B. Huang, *J. Comput. Chem.*, 2016, **37**, 825.
42 B. Huang, H. Dong, K.-L. Wong, L. Sun, and C. Yan, *J. Rare Earths*, 2017, **35**, 315.
43 N. J. J. Johnson, S. He, S. Diao, E. M. Chan, H. Dai, and A. Almutairi, *J. Am. Chem. Soc.*, 2017, **139**, 3275.
44 Q. Chen, et al., *Angew. Chem. Int. Ed.*, 2017, **56**, 7605.
45 J. Wang, et al., *Nat. Mater.*, 2014, **13**, 157.
46 F. Auzel, in *Radiationless Processes*, edited by B. DiBartolo and V. Goldberg (Springer US, Boston, MA, 1980), p. 213.
47 D. Yang, P. a. Ma, Z. Hou, Z. Cheng, C. Li, and J. Lin, *Chem. Soc. Rev.*, 2015, **44**, 1416.
48 S. J. Clark, M. D. Segall, C. J. Pickard, P. J. Hasnip, M. I. J. Probert, K. Refson, and M. C. Payne, *Zeitschrift Fur Kristallographie*, 2005, **220**, 567.
49 L. Kleinman and D. M. Bylander, *Phys. Rev. Lett.*, 1982, **48**, 1425.
50 S. G. Louie, S. Froyen, and M. L. Cohen, *Phys. Rev. B*, 1982, **26**, 1738.
51 I. Grinberg, N. J. Ramer, and A. M. Rappe, *Phys. Rev. B*, 2000, **62**, 2311.
52 A. M. Rappe, K. M. Rabe, E. Kaxiras, and J. D. Joannopoulos, *Phys. Rev. B*, 1990, **41**, 1227.
53 B. Huang, *Solid State Commun.*, 2016, **230**, 49.
54 B. Huang, *Inorg. Chem.*, 2015, **54**, 11423.
55 B. Huang, *Solid State Commun.*, 2016, **237–238**, 34.
56 B. Huang, *Phys. Chem. Chem. Phys.*, 2016, **18**, 13564.
57 B. Huang, R. Gillen, and J. Robertson, *J. Phys. Chem. C*, 2014, **118**, 24248.
58 B. Huang, *Philosophical Magazine*, 2014, **94**, 3052.
59 B. Huang and M. Sun, *Phys. Chem. Chem. Phys.*, 2017, **19**, 9457.
60 B. Huang, *Phys. Chem. Chem. Phys.*, 2017, **19**, 12683.
61 S. Hirata and M. Head-Gordon, *Chem. Phys. Lett.*, 1999, **314**, 291.
62 G. Chen, T. Y. Ohulchanskyy, A. Kachynski, H. Ågren, and P. N. Prasad, *ACS Nano*, 2011, **5**, 4981.
63 P. Dorenbos, *J. Lumin.*, 2004, **108**, 301.
64 P. Dorenbos, *Chem. Mater.*, 2005, **17**, 6452.
65 P. Dorenbos, *J. Alloy. Compd.*, 2009, **488**, 568.
66 C. Huang and Z. Bian, in *Rare Earth Coordination Chemistry* (John Wiley & Sons, Ltd, 2010), p. 1.
67 J. W. Stouwdam, M. Raudsepp, and F. C. J. M. van Veggel, *Langmuir.*, 2005, **21**, 7003.

TOC

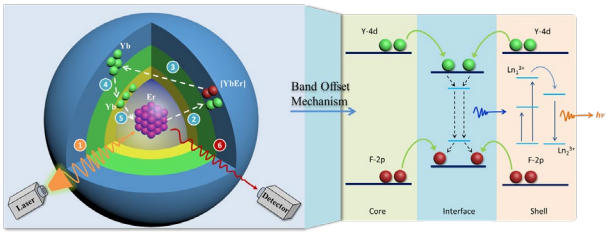

Synopsis (19 words)

The interplay on enhancing and quenching effects between Er^{3+} and Yb^{3+} dopant clusters in self-sensitized core@shell nanoparticles is studied.